# Generation of high-fidelity controlled-NOT logic gates by coupled superconducting qubits

Andrei Galiautdinov*

*Department of Physics and Astronomy, University of Georgia, Athens, Georgia 30602, USA*

(Received 16 January 2007; revised manuscript received 23 February 2007; published 2 May 2007)

Building on the previous results of the Weyl chamber steering method, we demonstrate how to generate high-fidelity controlled-NOT (CNOT) gates by direct application of certain physically relevant Hamiltonians with *fixed coupling constants* containing Rabi terms. Such Hamiltonians are often used to describe two superconducting qubits driven by local rf pulses. It is found that in order to achieve 100% fidelity in a system with *capacitive* coupling of strength $g$, one Rabi term suffices. We give the exact values of the physical parameters needed to implement such CNOT gates. The gate time and all possible Rabi frequencies are found to be $t=\pi/(2g)$ and $\Omega_1/g=\sqrt{64n^2-1}, n=1,2,3,\ldots$. Generation of a perfect CNOT gate in a system with *inductive* coupling, characterized by additional constant $k$, requires the presence of both Rabi terms. The gate time is again $t=\pi/(2g)$, but now there is an infinite number of solutions, each of which is valid in a certain range of $k$ and is characterized by a pair of integers $(n,m)$, $\frac{\Omega_{1,2}}{g}=\sqrt{16n^2-(\frac{k-1}{2})^2}\pm\sqrt{16m^2-(\frac{k+1}{2})^2}$. We distinguish two cases, depending on the sign of the coupling constant: (i) the *antiferromagnetic* case $(k\geqslant 0)$ with $n\geqslant m=0,1,2,\ldots$ and (ii) the *ferromagnetic* case $(k\leqslant 0)$ with $n>m=0,1,2,\ldots$. We conclude with consideration of fidelity degradation by switching to resonance. Simulation of time evolution based on the fourth-order Magnus expansion reveals characteristics of the gate similar to those found in the exact case, with slightly shorter gate time and shifted values of the Rabi frequencies.

DOI: 10.1103/PhysRevA.75.052303 PACS number(s): 03.67.Lx, 03.65.Fd, 85.25.−j

## I. INTRODUCTION

The goal of this paper is to show how to successfully generate, with a minimal amount of effort, a high-fidelity controlled-NOT (CNOT) gate in systems consisting of coupled superconducting qubits described by Hamiltonians with *coupling constants fixed by architecture*. We want to find out if making a CNOT gate in such systems can, at least theoretically, be reduced to a simple push of a button. Once initially set, the system itself would then take care of the needed gate by freely evolving from the identity of the unitary group to the target along the corresponding geodesic.

We thus approach the subject of time control from the "opposite," nonoptimal end. The plug-and-play implementations considered in this paper may be useful for simple gate designs which do not rely on sophisticated time control of their physical parameters. The question of simplicity will also become important once the best qubit is identified and put together with thousands of others to form an integrated circuit. Optimally controlling [1] qubits in such a circuit would become a difficult task, potentially leading to a compromise between the optimal and the simple. Thus, in this paper we limit our attention mostly to time-independent Hamiltonians. The only place where time dependence necessarily arises is in the analysis of fidelity degradation due to switching to resonance, considered in Sec. VI.

Two important developments motivated our work. The first was a series of experiments [2–4] which showed that the macroscopic quantum states [5,6] of Josephson junctions have coherence times long enough for such states to be used as qubits. That led to our choice of the physical Hamiltonians. The other development was the work on the Weyl chamber steering method [7,8] in which several examples of direct generation of various important gates, including CNOT gates, were considered from a purely geometrical standpoint.

In what follows we will use square brackets $[\cdots]$ to denote the gate—a representative of a given local class—located in a Weyl chamber.

## II. CONCEPT OF LOCAL EQUIVALENCE

We begin by recalling the notion of local equivalence within the special unitary group SU(4). Two gates $U_1$, $V_1 \in \mathrm{SU}(4)$ are *locally equivalent* if they differ only by local transformations:

$$U_1 \sim V_1 \Leftrightarrow U_1 = k_1 V_1 k_2, \quad k_1, k_2 \in \mathrm{SU}(2)\otimes\mathrm{SU}(2). \quad (1)$$

It is obvious that local equivalence is an example of the equivalence relation: it is reflexive $(U\sim U)$, symmetric $(U\sim V \Leftrightarrow V\sim U)$, and transitive $(U\sim V, V\sim W \Rightarrow U\sim W)$. When an equivalence relation is defined on a set, it partitions the set into disjoint classes. Thus, the entire group SU(4) is partitioned into classes of locally equivalent elements; any such element (a two qubit gate) belongs to one and only one local equivalence class.

To generalize the concept of local equivalence to the full U(4) we use the fact that any $U\in \mathrm{U}(4)$ can be written in the form $U=e^{i\alpha}U_1$, with $U_1\in\mathrm{SU}(4)$ [even though, as groups, $\mathrm{U}(4)\neq \mathrm{U}(1)\otimes\mathrm{SU}(4)$]. Then two gates $U=e^{i\alpha}U_1$ and $V=e^{i\beta}V_1\in\mathrm{U}(4)$ are locally equivalent if their representatives in SU(4) are equivalent:

$$U\sim V \Leftrightarrow U_1 \sim V_1. \quad (2)$$

One way to represent local classes in SU(4) is with the help of a Cartan decomposition of the underlying Lie algebra $L=\mathrm{su}(4)$. This can be seen as follows.

*Electronic address: ag@physast.uga.edu

 

For any *semisimple* Lie algebra $L$, its Cartan decomposition is a direct sum of two *subspaces* $L = K \oplus P$, one of which, $K$, is itself a Lie algebra, $[K,K] \subset K$, and the other, $P$, satisfies $[P,P] \subset K$, $[P,K] \subset P$. Because $K \cap P = 0$, any subalgebra $A \subset P$ must necessarily be Abelian. Such *maximal* Abelian subalgebra $A_C \subset P$ is called the Cartan subalgebra of $L$ relative to the given Cartan decomposition. An important Cartan decomposition theorem (for *groups*) states that if a semisimple algebra $L$ has decomposition $L = K \oplus P$, then any element $U_1 \in \exp L$ can always be written in the form

$$U_1 = k_1 V_1 k_2, \tag{3}$$

where $V_1 \in \exp A_C$ and $k_1, k_2 \in \exp K$.

An example of a Cartan decomposition is provided by su(2), for which we can take $K = \text{span}\{\frac{i}{2}\sigma_z\}$, $P = \text{span}\{\frac{i}{2}\sigma_x, \frac{i}{2}\sigma_y\}$, and $A_C = \text{span}\{\frac{i}{2}\sigma_x\}$.

Cartan decompositions of su(4) are more complicated, but a special choice [1] of $K$ spanned by the local operators

$$X_1 = \frac{i}{2}\sigma_x^1, \quad Y_1 = \frac{i}{2}\sigma_y^1, \quad Z_1 = \frac{i}{2}\sigma_z^1,$$

$$X_2 = \frac{i}{2}\sigma_x^2, \quad Y_2 = \frac{i}{2}\sigma_y^2, \quad Z_2 = \frac{i}{2}\sigma_z^2 \tag{4}$$

and $P$ spanned by all nonlocal operators $\frac{i}{2}\sigma_\alpha^1\sigma_\beta^2$ $(\alpha, \beta = x, y, z)$ is particularly useful. If we now take the span of mutually commuting operators

$$XX = \frac{i}{2}\sigma_x^1\sigma_x^2, \quad YY = \frac{i}{2}\sigma_y^1\sigma_y^2, \quad ZZ = \frac{i}{2}\sigma_z^1\sigma_z^2 \tag{5}$$

to serve as $A_C$, the Cartan decomposition theorem applied to $SU(4) = \exp[su(4)]$ gives

$$U_1 = k_1 \exp(c_1 XX + c_2 YY + c_3 ZZ) k_2. \tag{6}$$

This results in a convenient representation of SU(4) local equivalence classes by the *class vectors* $[c_1, c_2, c_3] \in A_C$. Representation of the U(4) classes is, up to phase, the same,

$$U = e^{i\alpha} k_1 \exp(c_1 XX + c_2 YY + c_3 ZZ) k_2. \tag{7}$$

The correspondence between class vectors and equivalence classes is *not* one to one: there are certain symmetries which map class vectors to other class vectors of the same equivalence class. However, it was shown in [7] that the correspondence can be made unique by restricting class vectors to a tetrahedral region in $A_C$, called a Weyl chamber. One such chamber, denoted by $a^\dagger$, is chosen to be canonical—it is described by the following three conditions [7,9]:

(i) $\pi > c_1 \geq c_2 \geq c_3 \geq 0$,
(ii) $c_1 + c_2 \leq \pi$,
(iii) if $c_3 = 0$, then $c_1 \leq \pi/2$.

Even though the choice of the Weyl chamber is not unique, when fixed, it becomes a powerful tool for analyzing time evolution on the full U(4).

In the original papers on the subject [7,8], several implementations of various useful gates by steering on $a^\dagger$ have been demonstrated. Of particular interest to us is the way $[\text{CNOT}] = [\pi/2, 0, 0] \in a^\dagger$ was generated by a *single* application of Hamiltonians with *controllable* Ising-type interaction, such as

$$H_{yy} = \Omega_{1x}\sigma_x^1 + \Omega_{2x}\sigma_x^2 + \Omega_{1z}\sigma_z^1 + \Omega_{2z}\sigma_z^2 + g\sigma_y^1\sigma_y^2, \tag{8}$$

and similarly for $H_{xx}, H_{zz}$. In [7,8], the local invariants of the corresponding unitary evolution $U(t) = \exp(iH_{yy}t)$ were first found in closed analytic form. Numerical analysis then produced the values for the time and the coupling constants needed to achieve a perfect [CNOT] in just one application.

Let us now turn to Hamiltonians used to describe coupled superconducting qubits. Such Hamiltonians may contain several Ising terms, which we choose to be fixed by architecture (cf. [10,11]). Our goal is to find out if they are also capable of generating [CNOT] in a single application, and if so, how many Rabi terms are required in order for such generation to be successful.

## III. HAMILTONIANS FOR COUPLED SUPERCONDUCTING QUBITS

When restricted to the two-qubit subspace, the Hamiltonian for two capacitively coupled phase qubits driven by rf pulses is given by

$$H_{\text{fast}} = \underbrace{-\sum_{i=1}^{2} \frac{\omega_i}{2}\sigma_z^i}_{H_0} + \underbrace{\sum_{i=1}^{2} \Omega_i \cos(\omega_{\text{rf}}^i t + \delta_i)\sigma_x^i + g\sigma_y^1\sigma_y^2}_{V}, \quad g > 0. \tag{9}$$

The level spacings $\omega_i$ are tunable between about 7 and 10 GHz. The Rabi frequencies $\Omega_i$ and the phases $\delta_i$ are fully controllable.

As it stands, this Hamiltonian is not suitable for actual gate implementations because of the very small time scale ($t_{\text{sc}} \sim 0.1$ ns) associated with $\omega_i$. The scale roughly corresponds to the time it takes to make a "round trip" on SU(4) when going in the direction of $-iH \in su(4)$. To attain high fidelity of the gate, we would have to control the pulses with accuracy which is experimentally unattainable.

To avoid this problem, the rotating-wave approximation (RWA) is used. We set the frequency of the external pulse to be equal to the transition frequency of the system (resonance), $\omega_{\text{rf}}^i = \omega_i \equiv \omega$, bring the phases to zero, and work in the interaction picture, in which the time evolution is governed by

$$H = e^{iH_0 t} V e^{-iH_0 t} = \sum_{i=1}^{2} \Omega_i \left[\cos^2(\omega t)\sigma_x^i + \frac{\sin(2\omega t)}{2}\sigma_y^i\right] + g[\cos(\omega t)\sigma_y^1 - \sin(\omega t)\sigma_x^1][\cos(\omega t)\sigma_y^2 - \sin(\omega t)\sigma_x^2]. \tag{10}$$

After averaging over fast oscillations the Hamiltonian becomes

$$H = \frac{\Omega_1}{2}\sigma_x^1 + \frac{\Omega_2}{2}\sigma_x^2 + \frac{g}{2}(\sigma_x^1\sigma_x^2 + \sigma_y^1\sigma_y^2) \tag{11}$$

or, in the language of Lie algebra su(4),

$$-iHt = -t[\Omega_1 X_1 + \Omega_2 X_2 + g(XX + YY)]. \tag{12}$$

There is an interesting modification of this qubit architecture based on inductive coupling between the qubits (see the Apendix). In that case an additional coupling constant $k$ is introduced, resulting in the full Hamiltonian

$$-iHt = -t[\Omega_1 X_1 + \Omega_2 X_2 + g(XX + YY + kZZ)]. \tag{13}$$

## IV. IMPLEMENTING [CNOT] BY TIME-INDEPENDENT HAMILTONIANS

### A. $XX+YY$ case

Here we show how to implement the perfect [CNOT] by a single application of the experimentally available Hamiltonian (12) with one Rabi term

$$-iHt = -t[\Omega_1 X_1 + g(XX + YY)]. \tag{14}$$

We first establish a useful group-theoretical property of the exponentials of Eq. (14). We consider a subalgebra of su(4), $A_0=\text{span}\{X_1, XX, YY, ZY\}$, whose generators obey the commutation relations summarized in the following:

| | $X_1$ | $XX$ | $YY$ | $ZY$ |
|---|---|---|---|---|
| $X_1$ | 0 | 0 | $-ZY$ | $YY$ |
| $XX$ | 0 | 0 | 0 | 0 |
| $YY$ | $ZY$ | 0 | 0 | $-X_1$ |
| $ZY$ | $-YY$ | 0 | $X_1$ | 0 |

. (15)

Notice that the $ZY$ generator had to be added to the set of generators in order to ensure closure under commutation.

The generator $XX$ is central in $A_0$. Its span is a one-dimensional Abelian ideal $I \subset A_0$, which makes $A_0$ into a *nonsemisimple* Lie algebra. This algebra is a direct sum of two subspaces, $A_0 = I \oplus A_1$, with $A_1 = \text{span}\{X_1, YY, ZY\}$ *isomorphic* to su(2).

Exponentiation of $A_0$ results in a *four*-dimensional subgroup $G_0 = \exp A_0 \subset \text{SU}(4)$ whose every element $W$ can be written as a product:

$$W = e^{-c_1 XX} \underbrace{e^{-\alpha X_1 - c_2 YY - bZY}}_{\text{an element of } \exp A_1}. \tag{16}$$

Because $A_1$ has its own Cartan decomposition (e.g., $A_1 = \text{span}\{X_1\} \oplus \text{span}\{YY, ZY\}$ with Cartan subalgebra $A_C = \text{span}\{YY\}$), application of the Cartan decomposition theorem to the group $G_1 = \exp A_1$ gives

$$W = e^{-c_1 XX} e^{-\alpha X_1} e^{-c_2 YY} e^{-\beta X_1}. \tag{17}$$

Now, because $e^{-iHt} = e^{-t[\Omega_1 X_1 + g(XX+YY)]}$ is itself an element of $G_0 = \exp A_0$, it can also be written as such product:

$$e^{-t[\Omega_1 X_1 + g(XX+YY)]} = e^{-\alpha X_1} e^{-c_1 XX - c_2 YY} e^{-\beta X_1}, \tag{18}$$

where the commutativity of $X_1$ and $XX$ has been used to rearrange the factors on the right.

Thus, given any gate $(t, \Omega_1, g)$ generated by $H$ in Eq. (14), with coupling $g$ fixed by architecture, there always exists a set of four numbers $(\alpha, c_1, c_2, \beta)$ which represent that gate exactly. This is essentially the same good old Cartan decomposition theorem (6) for SU(4), restricted to a physically relevant subgroup $G_0$ associated with the experimentally available Hamiltonian (14).

By fixing $\Omega_1$ and evolving the system freely under the action of its Hamiltonian, we generate a flow along a straight line in su(4) which has its image in both the Weyl chamber and the group SU(4).

The converse is unfortunately not necessarily true: for a given gate $(\alpha, c_1, c_2, \beta)$ it is not always possible to find $(t, \Omega_1)$ generating that gate. This is because of the noncommutativity between $X_1$ and $YY$.

Even though there is no guarantee that $H$ would be able to reach every $(c_1, c_2, 0)$ equivalence class in a single application, it is interesting to find out what actually *can* be reached. In particular, we want to know if [CNOT] is reachable.

It is obvious that if $\Omega_1 = 0$, then any local class with $c_1 = c_2$ and $c_3 = 0$ can be directly reached. What if $\Omega_1 \neq 0$?

Setting $\alpha = \beta = 0$ and directly exponentiating in Eq. (18) we get the matrix equation

$$\begin{bmatrix} \cos b_1 - \cos a & 0 & icd \sin a & i(\sin b_1 - d \sin a) \\ 0 & \cos b_2 - \cos a & i(\sin b_2 + d \sin a) & icd \sin a \\ icd \sin a & i(\sin b_2 + d \sin a) & \cos b_2 - \cos a & 0 \\ i(\sin b_1 - d \sin a) & icd \sin a & 0 & \cos b_1 - \cos a \end{bmatrix} = 0, \tag{19}$$

where

$$a = \frac{tg}{2}\sqrt{1+\left(\frac{\Omega_1}{g}\right)^2}, \quad b_{1,2} = \frac{1}{2}(tg - c_1 \pm c_2),$$
$$c = \frac{\Omega_1}{g}, \quad d = \frac{1}{\sqrt{1+\left(\frac{\Omega_1}{g}\right)^2}}. \tag{20}$$

If $\Omega_1 \neq 0$, then $\sin a = 0$, leading to $\cos a = \pm 1$ and $\cos b_1 = \cos b_2 = \pm 1$, $\sin b_{1,2} = 0$. This is only possible if $b_1 = b_2 + 2\pi m$ or

$$c_2 = 2\pi m, \quad m = 0,1,2,\ldots . \tag{21}$$

The minimal time solution is therefore

$$t_{\min} = \frac{c_1}{g},$$
$$\frac{\Omega_1}{g} = \sqrt{\left(\frac{4\pi n}{c_1}\right)^2 - 1}, \quad n = 1,2,3,\ldots . \tag{22}$$

Thus, by following $H$ along its geodesic for a time $t_{\min}$ we can (exactly) reach any equivalence class located on the $XX$ axis of the Weyl chamber. It is clear that the coupling constant $g$ plays the role of the scaling factor between the coordinate $c_1$ of the point on this axis and the actual, *physical* time required to reach that point.

We want to emphasize that the corresponding trajectory in the Weyl chamber is *not* a straight line from $O$ to [CNOT], even though is a straight line in the full Lie algebra su(4). This is because with $\Omega_1$ now being fixed by Eq. (22), it is not true that $e^{-t[\Omega_1 X_1 + g(XX+YY)]} \sim e^{-c_1(t)XX}$ is satisfied for all intermediate times $0 < t < t_{\min}$. In general for such times, $c_2(t) \neq 0$ in Eq. (18).

One important local class belonging to the $XX$ axis is [CNOT], which can be made by exponentiating the Hamiltonian $-iH_{[\mathrm{CNOT}]}t = -tXX$ with $t = \pi/2$. The corresponding matrix in the computational basis is

$$[\mathrm{CNOT}] = \exp\left(-\frac{\pi}{2}XX\right) = \frac{1}{\sqrt{2}}\begin{bmatrix} 1 & 0 & 0 & -i \\ 0 & 1 & -i & 0 \\ 0 & -i & 1 & 0 \\ -i & 0 & 0 & 1 \end{bmatrix} \in \mathrm{SU}(4). \tag{23}$$

The Makhlin invariants [12] of this [CNOT] are $G_1 = 0$ and $G_2 = 1$, as required, so this is a perfectly acceptable [CNOT] out of which the canonical CNOT gate with matrix

$$\mathrm{CNOT} = \begin{bmatrix} 1 & 0 & 0 & 0 \\ 0 & 1 & 0 & 0 \\ 0 & 0 & 0 & 1 \\ 0 & 0 & 1 & 0 \end{bmatrix} \in \mathrm{U}(4) \tag{24}$$

can be produced by local manipulation of individual qubits. We will give some examples of the needed for this local rf pulses in Sec. V.

Thus, setting $c_1 = \pi/2$ in Eq. (22), we get

$$t_{\min} = \pi/(2g),$$
$$\Omega_1/g = \sqrt{64n^2 - 1}, \quad n = 1,2,3,\ldots . \tag{25}$$

The simplest exact [CNOT] is then

$$[\mathrm{CNOT}] = e^{-(\pi/2g)[\sqrt{63}gX_1 + g(XX+YY)]}. \tag{26}$$

For completeness we mention another [CNOT] solution to Eq. (18),

$$\Omega_1/g = \sqrt{16n^2 - 1}, \quad n = 1,2,3,\ldots, \tag{27}$$

which is *up-to-phase* geodesic,

$$[\mathrm{CNOT}] = e^{2\pi X_1} e^{-(\pi/2g)[\Omega_1 X_1 + g(XX+YY)]}. \tag{28}$$

### B. $XX+YY+kZZ$ case

We are now going to show that a single application of the Hamiltonian given in Eq. (13) generates the exact [CNOT], provided both Rabi terms are kept.

Derivation parallels the previous case. We concentrate on subalgebra $A_0 \subset \mathrm{su}(4)$:

| | $X_1$ | $X_2$ | $XX$ | $YY$ | $ZZ$ | $YZ$ | $ZY$ |
|---|---|---|---|---|---|---|---|
| $X_1$ | 0 | 0 | 0 | $-ZY$ | $YZ$ | $-ZZ$ | $YY$ |
| $X_2$ | 0 | 0 | 0 | $-YZ$ | $ZY$ | $YY$ | $-ZZ$ |
| $XX$ | 0 | 0 | 0 | 0 | 0 | 0 | 0 |
| $YY$ | $ZY$ | $YZ$ | 0 | 0 | 0 | $-X_2$ | $-X_1$ |
| $ZZ$ | $-YZ$ | $-ZY$ | 0 | 0 | 0 | $X_1$ | $X_2$ |
| $YZ$ | $ZZ$ | $-YY$ | 0 | $X_1$ | $-X_1$ | 0 | 0 |
| $ZY$ | $-YY$ | $ZZ$ | 0 | $X_1$ | $-X_2$ | 0 | 0 |

. (29)

The generator $XX$ is again central in $A_0$, spanning a one-dimensional Abelian ideal $I \subset A_0$. This makes $A_0$ into a non-semisimple Lie algebra which is a direct sum of two subspaces, $A_0 = I \oplus A_1$, where $A_1 = \mathrm{span}\{X_1, X_2, YY, ZZ, YZ, ZY\}$.

Exponentiation of $A_0$ results in a *seven*-dimensional subgroup $G_0 = \exp A_0 \subset \mathrm{SU}(4)$ whose every element $W$ can be written as a product:

$$W = e^{-c_1 XX} \underbrace{e^{-aX_1 - bX_2 - c_2 YY - c_3 ZZ - dYZ - fZY}}_{\text{an element of } \exp A_1}. \tag{30}$$

Because $A_1$ has its own Cartan decomposition (e.g., $A_1 = \mathrm{span}\{X_1, X_2\} \oplus \mathrm{span}\{YY, ZZ, YZ, ZY\}$ with a Cartan subalgebra $A_C = \mathrm{span}\{YY, ZZ\}$), application of the Cartan decomposition theorem to the group $G_1 = \exp A_1$ gives

$$W = e^{-c_1 XX} e^{-\alpha X_1 - \beta X_2} e^{-c_2 YY - c_3 ZZ} e^{-\eta X_1 - \xi X_2}. \tag{31}$$

Since $e^{-iHt} = e^{-t[\Omega_1 X_1 + \Omega_2 X_2 - g(XX+YY+kZZ)]}$ is itself an element of $G_0 = \exp A_0$, it can also be written as such product

$$e^{-t[\Omega_1 X_1 + \Omega_2 X_2 + g(XX+YY+kZZ)]} = e^{-\alpha X_1 - \beta X_2} e^{-c_1 XX - c_2 YY - c_3 ZZ} e^{-\eta X_1 - \xi X_2}. \tag{32}$$

Thus, given any gate $(t, \Omega_1, \Omega_2, g, k)$ generated by $H$ in Eq. (13), with couplings $g$ and $k$ fixed by architecture, there always exists a set of seven numbers $(\alpha,\beta,c_1,c_2,c_3,\eta,\xi)$ which represent that gate exactly. This is again the Cartan decomposition theorem for SU(4), this time restricted to a physically relevant subgroup $G_0$ associated with the experimentally available Hamiltonian (13).

With $\alpha=\beta=\eta=\xi=0$, Eq. (32) has an infinite number of minimal time solutions labeled by pairs of integers $(n,m)$ and valid in certain intervals of $k$:

$$t_{\min}=\frac{c_1}{g},$$

$$\frac{\Omega_{1,2}}{g}=\sqrt{\left(\frac{2\pi n}{c_1}\right)^2-\left(\frac{k-1}{2}\right)^2}\pm\sqrt{\left(\frac{2\pi m}{c_1}\right)^2-\left(\frac{k+1}{2}\right)^2}. \tag{33}$$

For [CNOT], $(c_1,c_2,c_3)=(\pi/2,0,0)$, which gives

$$t_{\min}=\pi/2g,$$

$$\frac{\Omega_{1,2}}{g}=\sqrt{16n^2-\left(\frac{k-1}{2}\right)^2}\pm\sqrt{16m^2-\left(\frac{k+1}{2}\right)^2}. \tag{34}$$

Two cases will be distinguished here, depending on the sign of the coupling constant.

### 1. kZZ coupling of antiferromagnetic type

In this case, $k\geqslant 0$ and $n\geqslant m=0,1,2,3,\ldots$. The previous result for $k=0$ is correctly recovered when $n=m=0$. For $n=m=1,2,\ldots$ we get an $(n,n)$th solution valid in the interval $0\leqslant k\leqslant 8n-1$.

Below, we list Rabi frequencies required to generate a *perfect plug-and-play* [CNOT] in the antiferromagnetic case for several values of $n$ and $m$:

| $k$ | $\Omega_1^{(1,1)}/g$ | $\Omega_2^{(1,1)}/g$ | $\Omega_1^{(2,1)}/g$ | $\Omega_2^{(2,1)}/g$ | $\Omega_1^{(2,2)}/g$ | $\Omega_2^{(2,2)}/g$ | $\Omega_1^{(3,3)}/g$ | $\Omega_2^{(3,3)}/g$ | |
|---|---|---|---|---|---|---|---|---|---|
| 0.00 | 7.937254 | 0.000000 | 11.952987 | 4.015733 | 15.968719 | 0.000000 | 23.979157 | 0.000000 | |
| 0.10 | 7.936614 | 0.012600 | 11.949341 | 4.025327 | 15.968405 | 0.006262 | 23.978949 | 0.004170 | |
| 0.25 | 7.933253 | 0.031513 | 11.942076 | 4.040336 | 15.966755 | 0.015658 | 23.977852 | 0.010426 | |
| 0.50 | 7.921238 | 0.063121 | 11.925151 | 4.067034 | 15.960859 | 0.031327 | 23.973935 | 0.020856 | |
| 1.00 | 7.872983 | 0.127017 | 11.872983 | 4.127017 | 15.937254 | 0.062746 | 23.958261 | 0.041739 | |
| 3.00 | 7.337085 | 0.408882 | 11.401356 | 4.473152 | 15.683221 | 0.191287 | 23.790420 | 0.126101 | |
| 5.00 | 6.109853 | 0.818350 | 10.391718 | 5.100215 | 15.162165 | 0.329768 | 23.451110 | 0.213209 | |
| 7.00 | 2.645751 | 2.645751 | 7.416198 | 7.416198 | 14.344402 | 0.487995 | 22.932659 | 0.305242 | (35) |
| 9.00 | | | | | 13.173201 | 0.683205 | 22.222421 | 0.404996 | |
| 11.00 | | | | | 11.536501 | 0.953495 | 21.301017 | 0.516407 | |
| 13.00 | | | | | 9.164486 | 1.418519 | 20.139099 | 0.645511 | |
| 15.00 | | | | | 3.872983 | 3.872983 | 18.691066 | 0.802522 | |
| 17.00 | | | | | | | 16.881526 | 1.007018 | |
| 19.00 | | | | | | | 14.570504 | 1.304004 | |
| 21.00 | | | | | | | 11.429081 | 1.837418 | |
| 23.00 | | | | | | | 4.795832 | 4.795832 | |

Notice that the product of Rabi frequencies for solutions of $(n,n)$ type is always equal to $k$:

$$\Omega_1^{(n,n)}\Omega_2^{(n,n)}/g^2=k. \tag{36}$$

### 2. kZZ coupling of ferromagnetic type

In this case, $k\leqslant 0$ and $n>m=0,1,2,\ldots$. A particularly interesting family of solutions occurs for $m=0$. These solutions [cf. Eq. (27)] exist only for the coupling constant $k=-1$:

$$\Omega_{1,2}^{(n,0)}/g=\sqrt{16n^2-1},\quad n=1,2,3,\ldots\;. \tag{37}$$

For certain $n>m=1,2,3$ we find

| $k$ | $\Omega_1^{(2,1)}/g$ | $\Omega_2^{(2,1)}/g$ | $\Omega_1^{(3,1)}/g$ | $\Omega_2^{(3,1)}/g$ | $\Omega_1^{(3,2)}/g$ | $\Omega_2^{(3,2)}/g$ |
|---|---|---|---|---|---|---|
| −0.00 | 11.952987 | 4.015733 | 15.958206 | 8.020952 | 19.973939 | 4.005219 |
| −0.10 | 11.955678 | 4.006464 | 15.961996 | 8.012782 | 19.974723 | 4.000055 |
| −0.25 | 11.957932 | 3.993165 | 15.966096 | 8.001330 | 19.974919 | 3.992507 |
| −0.50 | 11.956946 | 3.972586 | 15.968719 | 7.984360 | 19.972632 | 3.980447 |
| −1.00 | 11.937254 | 3.937254 | 15.958261 | 7.958261 | 19.958261 | 3.958261 |
| −2.00 | 11.826744 | 3.889490 | 15.874508 | 7.937254 | 19.890241 | 3.921521 |
| −3.00 | 11.618950 | 3.872983 | 15.705143 | 7.959176 | 19.769413 | 3.894906 |
| −4.00 | 11.307441 | 3.891243 | 15.444795 | 8.028595 | 19.594811 | 3.878578 |
| −5.00 | 10.880300 | 3.952097 | 15.083052 | 8.154848 | 19.364917 | 3.872983 |
| −6.00 | 10.316246 | 4.071248 | 14.600739 | 8.355741 | 19.077582 | 3.878898 |
| −7.00 | 9.573955 | 4.282452 | 13.959460 | 8.667957 | 18.729907 | 3.897510 |
| −8.00 | 8.550870 | 4.677887 | 13.060789 | 9.187806 | 18.318045 | 3.930550 |
| −9.00 | 6.244998 | 6.244998 | 10.908712 | 10.908712 | 17.836915 | 3.980509 |
| −11.00 | | | | | 16.637303 | 4.147307 |
| −13.00 | | | | | 15.038297 | 4.455292 |
| −15.00 | | | | | 12.817255 | 5.071289 |
| −17.00 | | | | | 7.937254 | 7.937254 |

(38)

## V. LOCAL rf PULSES

Here we give two (ideal) local rf-pulse sequences needed to produce the true, canonical CNOT gate from the [CNOT] located in the Weyl chamber via

$$\text{CNOT} = e^{i\pi/4}k_1[\text{CNOT}]k_2. \tag{39}$$

*Sequence 1*. Total rotation $\varphi = 3\pi/2$,

$$k_1 = e^{-(\pi/2)Y_1}e^{(\pi/2)(X_1 - X_2)}, \quad k_2 = e^{(\pi/2)Y_1}. \tag{40}$$

*Sequence 2*. Total rotation $\varphi = 3\pi/2$,

$$k_1 = e^{-(\pi/2)Y_1}, \quad k_2 = e^{-(\pi/2)Z_1}e^{(\pi/2)(X_1 - X_2)}. \tag{41}$$

## VI. FIDELITY DEGRADATION BY SWITCHING TO RESONANCE

We are now going to consider the effect of switching—the actual process of bringing the qubits to resonance with an external rf field.

We will assume that [CNOT] generation is performed in three stages.

*Stage 1: tuning*. Very fast linear rise of Rabi frequencies to their optimal values (for a given $k$), with time-dependent Hamiltonian

$$-iH_{\text{tune}} = -\left[(\Omega_1^{\text{opt}}X_1 + \Omega_2^{\text{opt}}X_2)\frac{t}{\epsilon t_{\text{gate}}} + g(XX + YY + kZZ)\right], \tag{42}$$

where $\epsilon \ll 1$ characterizes the fraction of the total gate time spent in the switching mode (tune and detune). We denote the corresponding time evolution by $U_{\text{tune}}$.

*Stage 2: resonance*. Evolution with optimal Rabi frequencies for the most part of [CNOT] generation, $U_{\text{resonance}}$, where

$$U_{\text{resonance}} = e^{-i(1-2\epsilon)t_{\text{gate}}H_{\text{resonance}}},$$

$$-iH_{\text{resonance}} = -[\Omega_1^{\text{opt}}X_1 + \Omega_2^{\text{opt}}X_2 + g(XX + YY + kZZ)]. \tag{43}$$

*Stage 3: detuning*. Fast linear decrease of Rabi frequencies to zero, with time-dependent Hamiltonian

$$-iH_{\text{detune}} = -\left[(\Omega_1^{\text{opt}}X_1 + \Omega_2^{\text{opt}}X_2)\left(1 - \frac{t}{\epsilon t_{\text{gate}}}\right) + g(XX + YY + kZZ)\right]. \tag{44}$$

The full gate is then the product

$$[\text{CNOT}]_{\text{opt}} = U_{\text{detune}}U_{\text{resonance}}U_{\text{tune}}. \tag{45}$$

In order to find the optimal values of the gate parameters, we first truncate the Magnus expansion for each switching part of the gate:

$$U_{\text{switching}}(\epsilon t_{\text{gate}}) = e^{\sigma(\epsilon t_{\text{gate}})}, \tag{46}$$

with

$$\sigma(\epsilon t_{\text{gate}}) \approx -i\int_0^{\epsilon t_{\text{gate}}} dt H_{\text{switching}}(t) + \frac{(-i)^2}{2}\int_0^{\epsilon t_{\text{gate}}} dt_1 \left[ H_{\text{switching}}(t_1), \times \int_0^{t_1} dt_2 H_{\text{switching}}(t_2) \right], \tag{47}$$

and then use the fourth-order iteration method [13]:

$$U_{n+1} = e^{\sigma_n} U_n,$$

$$\sigma_n = \frac{h}{2}(A_1 + A_2) + \frac{\sqrt{3}h^2}{12}[A_1, A_2],$$

$$A_1 = -iH_{\text{switching}}(t_n + c_1 h),$$

$$A_2 = -iH_{\text{switching}}(t_n + c_2 h),$$

$$h = \frac{\epsilon t_{\text{gate}}}{N}, \tag{48}$$

where $N$ is the number of iteration steps and

$$c_{1,2} = \frac{1}{2} \pm \frac{\sqrt{6}}{3} \tag{49}$$

are the nodes of the Gauss-Legandre fourth-order quadrature in [0, 1]. As described in [13], despite the presence of only $h$ and $h^2$ terms, this is indeed the fourth-order approximation to the Magnus expansion.

Optimization of the gate's parameters was performed using a Nelder-Mead simplex direct search with bound constraints [14] for the minimum of the square of the Frobenius distance,

$$d^2_{\text{Frobenius}} = \text{tr}[([\text{CNOT}] - [\text{CNOT}]_{\text{opt}})^\dagger([\text{CNOT}] - [\text{CNOT}]_{\text{opt}})], \tag{50}$$

between the optimal $[\text{CNOT}]_{\text{opt}}$ given by Eq. (45) and the perfect [CNOT] given in Eq. (23). Due to the enormous richness of possible CNOTs, we optimized only the most interesting of them. With $N$=2500 we simulated the switching mechanism for $\epsilon$=0.025:

| $k$ | $\Omega_1^{\text{opt}}/g$ | $\Omega_2^{\text{opt}}/g$ | $t_{\text{gate}}$ [units of $\pi/(2g)$] | $d^2_{\text{Frobenius}}$ [units of $10^{-3}$] |
|---|---|---|---|---|
| 0.50 | 8.130446 | 0.064667 | 0.999268 | 1.9 |
| 0.25 | 8.141971 | 0.032287 | 0.999363 | 1.6 |
| 0.10 | 8.145193 | 0.012910 | 0.999390 | 1.5 |
| 0.00 | 8.145807 | 0.000000 | 0.999395 | 1.5 |
| −0.10 | 12.269887 | 4.111716 | 0.999382 | 1.5 |
| −0.25 | 12.272602 | 4.098223 | 0.999348 | 1.6 |
| −0.50 | 12.272970 | 4.077597 | 0.999237 | 1.9 |

(51)

Using the local pulses given in Sec. V we can transform the corresponding optimal $[\text{CNOT}]_{\text{opt}}$ to its canonical form. For example,

$$\text{CNOT}_{k=0.25} = \begin{bmatrix} 0.9998 - 0.0025i & -0.0001 - 0.0017i & -0.0001 - 0.0047i & 0.0192i \\ -0.0001 - 0.0017i & 0.9998 - 0.0025i & -0.0193i & 0.0001 + 0.0047i \\ 0.0193i & 0.0047i & 0.0001 - 0.0007i & 0.9998 + 0.0025i \\ -0.0001 - 0.0047i & -0.0192i & 0.9998 + 0.0025i & 0.0001 - 0.0007i \end{bmatrix}, \tag{52}$$

whose intrinsic fidelity relative to the computational basis is

$$F = \frac{1}{4}\sum_{r=1}^{4} |(\text{CNOT}^\dagger \times \text{CNOT}_{k=0.25})_{rr}| = 0.9998. \tag{53}$$

## VII. CONCLUSION

To recapitulate, we have demonstrated how to implement various high-fidelity, plug-and-play CNOT logic gates by a single application of Hamiltonians used to describe coupled superconducting qubits. Architectures involving capacitive and inductive couplings have been analyzed for which the physical parameters required to generate the perfect CNOT gate have been found in closed, analytic form. Additional numerical simulations based on fourth-order Magnus expansion were used to correct this ideal limit by taking into account the switching to resonance.

## ACKNOWLEDGMENTS

This work was supported by the Disruptive Technology Office under Grant No. W911NF-04-1-0204 and by the National Science Foundation under Grant No. CMS-0404031. The author would like to thank Michael Geller, Emily Pritchett, and Andrew Sornborger for helpful discussions.


## APPENDIX: DERIVATION OF THE HAMILTONIAN FOR INDUCTIVELY COUPLED FLUX QUBITS

The system consists of two superconducting loops of self-inductance $L$ coupled by a mutual inductance $M$ and driven by external magnetic fluxes $\Phi_i$, as shown in Fig. 1. Each loop is interrupted by a Josephson junction of critical current $I_0$ and effective capacitance $C$.

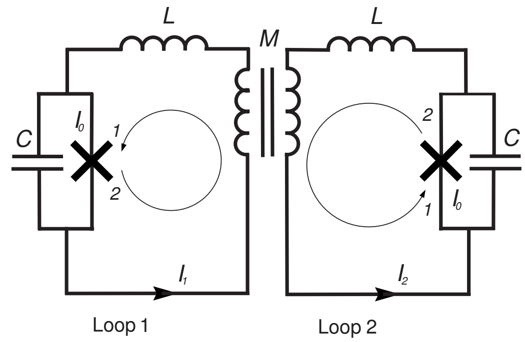


FIG. 1. Circuit diagram for a system consisting of two inductively coupled flux qubits.

Inside the superconducting material, the Ginzburg-Landau complex order parameter can be written in the usual form

$$\psi(\mathbf{r}) = \sqrt{\rho_s(\mathbf{r})}e^{i\theta(\mathbf{r})}, \tag{A1}$$

where $\rho_s$ is the density of Cooper pairs. The supercurrent flux is

$$\mathbf{j}_s = \frac{\hbar\rho_s}{m^*}\left(\boldsymbol{\nabla}\theta - \frac{q}{\hbar}\mathbf{A}_s\right), \tag{A2}$$

where $\mathbf{A}_s$ is the vector potential inside the superconductor and $q=-2e$. The gauge is assumed to be chosen in such a way as to guarantee $\hat{\mathbf{n}}\cdot\mathbf{j}_s=\mathbf{0}$ at the surface. In the clean limit, $\mathbf{j}_s=\mathbf{0}$ inside the material, which leads to

$$\mathbf{A}_s = \frac{\hbar}{q}\boldsymbol{\nabla}\theta. \tag{A3}$$

The line integral of $\mathbf{A}$ around loop 1 is (here, the limits of integrations 1 and 2 denote the two sides of the junction; the rest of notation is clear from the context)

$$\begin{aligned}
\oint_{\text{loop 1}} \mathbf{A}\cdot d\mathbf{l} &= \left(\int_1^2 \mathbf{A}\cdot d\mathbf{l}\right)_{\text{inside JJ}} + \left(\int_2^1 \mathbf{A}\cdot d\mathbf{l}\right)_{\text{in the rest of circuit (inside superconducting bulk)}} \\
&= \left[\int_1^2 \mathbf{A}_{\text{JJ}}\cdot d\mathbf{l} - \frac{\hbar}{q}(\theta_2-\theta_1)\right] + \left[\frac{\hbar}{q}(\theta_2-\theta_1) - \int_1^2 \mathbf{A}_s\cdot d\mathbf{l}\right] \\
&= -\frac{\hbar}{q}\left[(\theta_2-\theta_1) - \frac{q}{\hbar}\int_1^2 \mathbf{A}_{\text{JJ}}\cdot d\mathbf{l}\right] - \frac{\hbar}{q}\left[(\theta_1-\theta_2) + \int_1^2 \boldsymbol{\nabla}\theta\cdot d\mathbf{l}\right] = -\frac{\hbar}{q}\left[\phi_1 + \oint_{\text{loop 1}} \boldsymbol{\nabla}\theta\cdot d\mathbf{l}\right] \\
&= -\frac{\hbar}{q}(\phi_1 + 2\pi n_1),
\end{aligned} \tag{A4}$$

where $\phi_1$ is the gauge-invariant phase difference across the first junction and $n_1=0,1,2,3,\ldots$. This "quantization" condition is justified by the fact that the order parameter is nonzero inside the junction [15]. Alternatively,

$$\oint_{\text{loop 1}} \mathbf{A}\cdot d\mathbf{l} = \Phi_1^{\text{external}} + \Phi_1^{\text{self}} + \Phi_1^{\text{mutual}} = \Phi_1 - LI_1 + MI_2. \tag{A5}$$

Introducing

$$\alpha = \frac{\hbar}{2e} = \frac{\Phi_{\text{sc}}}{2\pi}, \quad E_J = \alpha I_0, \quad \omega_0 = \frac{1}{\sqrt{LC}}, \quad E_0 = \frac{\alpha^2}{L} = \frac{\hbar^2\omega_0^2}{2E_C},$$

$$E_C = \frac{(2e)^2}{2C}, \quad \Upsilon = \frac{M}{L}, \tag{A6}$$

and taking into account Eqs. (A4) and (A5) together with the Josephson equations, we get the equations of motion for the two gauge-invariant phase differences:

$$\alpha^2 C(\ddot{\phi}_1 - \Upsilon\ddot{\phi}_2) = -E_J(\sin\phi_1 - \Upsilon\sin\phi_2) - E_0\left(\phi_1 + 2\pi n_1 - \frac{2\pi\Phi_1}{\Phi_{\text{sc}}}\right),$$

$$\alpha^2 C(\ddot{\phi}_2 - \Upsilon \ddot{\phi}_1) = - E_J(\sin \phi_2 - \Upsilon \sin \phi_1) - E_0\left(\phi_2 + 2\pi n_2 - \frac{2\pi\Phi_2}{\Phi_{sc}}\right). \quad (A7)$$

It is clear that $2\pi n_i$ are not dynamical and can be absorbed into $\phi_i + 2\pi n_i \rightarrow \phi_i$ without affecting any physics. Notice also that in the limit $M \rightarrow 0$ we correctly recover a well-known result for two independent loops.

Because of the presence of terms $\Upsilon E_J \sin \phi_i$ in Eq. (A7), we cannot immediately deduce the system's Lagrangian. However, by multiplying the second equation Eqs. (A7) by $\Upsilon$ and by adding the result to the first equation, we can separate the variables:

$$\alpha^2 C(1-\Upsilon^2)\ddot{\phi}_1 = - E_J(1-\Upsilon^2)\sin \phi_1 - E_0\left[\left(\phi_1 - \frac{2\pi\Phi_1}{\Phi_{sc}}\right) + \Upsilon\left(\phi_2 - \frac{2\pi\Phi_2}{\Phi_{sc}}\right)\right], \quad (A8)$$

and similarly for $\ddot{\phi}_2$. The Lagrangian is now easily found to be

$$L = (1-\Upsilon^2)\left\{\frac{\alpha^2 C}{2}(\dot{\phi}_1^2 + \dot{\phi}_2^2) + E_J(\cos \phi_1 + \cos \phi_2)\right\} - \frac{E_0}{2}\left[\left(\phi_1 - \frac{2\pi\Phi_1}{\Phi_{sc}}\right)^2 + \left(\phi_2 - \frac{2\pi\Phi_2}{\Phi_{sc}}\right)^2\right] - \Upsilon E_0\left(\phi_1 - \frac{2\pi\Phi_1}{\Phi_{sc}}\right)\left(\phi_2 - \frac{2\pi\Phi_2}{\Phi_{sc}}\right). \quad (A9)$$

In the limit of weak coupling ($\Upsilon \ll 1$) the terms $\sim\Upsilon^2$ can be dropped, giving

$$H = \frac{p_1^2 + p_2^2}{2m} + U(\phi_1, \phi_2), \quad (A10)$$

with $p_i = m\dot{\phi}_i$, $m = \alpha^2 C$, and

$$U(\phi_1, \phi_2) = \sum_{i=1}^{2}\left[- E_J \cos \phi_i + \frac{E_0}{2}\left(\phi_i - \frac{2\pi\Phi_i}{\Phi_{sc}}\right)^2\right] + \Upsilon E_0\left(\phi_1 - \frac{2\pi\Phi_1}{\Phi_{sc}}\right)\left(\phi_2 - \frac{2\pi\Phi_2}{\Phi_{sc}}\right). \quad (A11)$$

After projecting onto the qubit subspace and using the RWA we recover Eq. (13).


[1] N. Khaneja, R. Brockett, and S. J. Glaser, Phys. Rev. A **63**, 032308 (2001).

[2] M. H. Devoret, J. M. Martinis, and J. Clarke, Phys. Rev. Lett. **55**, 1908 (1985); J. M. Martinis, M. H. Devoret, and J. Clarke, Phys. Rev. B **35**, 4682 (1987); J. Clarke *et al.*, Science **239**, 992 (1988); J. M. Martinis, S. Nam, J. Aumentado, and C. Urbina, Phys. Rev. Lett. **89**, 117901 (2002); J. M. Martinis *et al.*, e-print cond-mat/0507622.

[3] P. R. Johnson, F. W. Strauch, A. J. Dragt, R. C. Ramos, C. J. Lobb, J. R. Anderson, and F. C. Wellstood, Phys. Rev. B **67**, 020509(R) (2003); A. Blais, A. Maassenvanden Brink, and A. M. Zagoskin, Phys. Rev. Lett. **90**, 127901 (2003).

[4] For a comprehensive review see M. H. Devoret, A. Wallraff, and J. M. Martinis, e-print cond-mat/0411174.

[5] A. J. Leggett, Suppl. Prog. Theor. Phys. **69**, 80 (1980).

[6] A. O. Caldeira and A. J. Leggett, Ann. Phys. (N.Y.) **149**, 374 (1983).

[7] J. Zhang, J. Vala, S. Sastry, and K. B. Whaley, Phys. Rev. A **67**, 042313 (2003).

[8] J. Zhang and K. B. Whaley, Phys. Rev. A **71**, 052317 (2005).

[9] R. R. Tucci, e-print quant-ph/0507171.

[10] B. L. T. Plourde *et al.*, Phys. Rev. B **70**, 140501(R) (2004).

[11] A. G. Kofman, Q. Zhang, J. M. Martinis, and A. N. Korotkov, e-print cond-mat/0606078.

[12] Yu. Makhlin, Quantum Inf. Process. **1**, 243 (2003).

[13] A. Iserles, A. Marthinsen, and S. P. Nørsett, BIT Numeri. Mathe. **39**, 281 (1999).

[14] This modification of the standard simplex search implementation for MATLAB is due to John D'Errico. It can be found at http://www.mathworks.com/matlabcentral/fileexchange.

[15] D. A. Jacobson, Phys. Rev. **138**, A1066 (1965).